

Electronic Structure Modulation and Photocatalytic Evaluation of Graphene-Based Systems: A Density Functional Theory Approach

Lekshmi Priya S¹, Remya Muralimanohar², Suchithra S³,
Saravana Kumar S⁴

^{1,2,4}PG and Research Department of Physics, NSS College, Pandalam, Kerala, India

³PG Department of Physics, St. Stephen's College, Pathanapuram, Kerala, India

Abstract

This study presents a theoretical investigation of the photocatalytic behavior of pristine and modified carbon-based systems, including TiO₂, graphene nanoplatelets, and TiO₂/graphene nanocomposites. Using Density Functional Theory (DFT), we analyzed the electronic properties—band structure, density of states (DOS), and charge density—of pristine graphene and various doped graphene systems (B-doped, N-doped, and Co-adsorbed graphene). Theoretical insights confirmed the role of dopants and heterojunctions in modulating electronic structure and enhancing charge separation. These findings highlight the promise of graphene-based modifications for high-efficiency photocatalysis.

Keywords: Density Functional theory, Density of States, band Structure, Photocatalytic Activity

1. Introduction

Human activities have led to severe ecological crises through air pollution, untreated wastewater discharge, and reliance on fossil fuels, which account for over 80% of global energy production [1]. These practices intensify greenhouse gas emissions and climate change, while conventional purification methods such as adsorption and membrane filtration remain energy-intensive and produce secondary pollutants [2]. Photocatalysis, often described as the “Holy Grail of science,” offers a promising alternative by using solar energy to degrade contaminants without harmful by-products [3]. Graphene, discovered in 2004, has gained prominence due to its large surface area, exceptional conductivity, and ability to enhance charge separation, making it highly effective in photocatalysis and adsorption [4]. When combined with TiO₂, graphene improves visible-light absorption and reduces recombination losses, addressing the limitations of TiO₂ such as wide bandgap and poor charge transport [5].

Defect engineering and heteroatom doping in graphene (e.g., N, B, Co) introduce localized energy states that extend light absorption into the visible spectrum, suppress charge recombination, and significantly boost photocatalytic performance [6]. Graphene/TiO₂ composites synthesized via hydrothermal or self-assembly methods show enhanced durability, scalability, and environmental compatibility. Computational modeling through Density Functional Theory (DFT) using Quantum ESPRESSO supports these findings, enabling precise analysis of electronic structures and defect-induced modifications [3]. By integrating DFT simulations with experimental photocatalysis studies, this work aims to bridge theoretical insights

with practical applications, contributing to the development of next-generation graphene-based photocatalysts with superior efficiency and sustainability [5].

2. Materials and Methods

The computational study employed Density Functional Theory (DFT) using the Quantum ESPRESSO package to investigate pristine, B-doped, N-doped, and Co-doped graphene systems [7]. A 4×4 supercell of graphene with vacuum spacing of 15 Å was constructed, and structural optimization was carried out until residual atomic forces were minimized. Boron substitution introduced hole states in the electronic structure, while nitrogen doping generated donor states indicative of n-type behavior. Cobalt was adsorbed at the hollow site of the graphene lattice, enabling the study of spin polarization and magnetic effects consistent with earlier reports. The Perdew–Burke–Ernzerhof (PBE) functional within the Generalized Gradient Approximation was used to describe exchange–correlation effects [8], and ultrasoft pseudopotentials with carefully chosen plane-wave cutoffs and k-point sampling ensured computational accuracy while maintaining efficiency.

The simulations revealed significant changes in graphene’s electronic properties arising from doping and transition-metal incorporation. Band structure calculations along the Γ –M–K– Γ path demonstrated Fermi level shifts, bandgap modulation, and mid-gap state formation. These results confirmed that boron and nitrogen alter the electronic character through acceptor and donor states, respectively [9]. Charge density mapping indicated localized redistribution and interfacial electron transfer, particularly in Co-doped graphene, where spin polarization produced notable magnetic effects [10]. The density of states further identified orbital contributions of dopants, linking heteroatom substitution to enhanced catalytic and conductive behavior. Together, these findings highlight the role of defect engineering in tuning graphene’s band structure and charge dynamics, reinforcing its potential in photocatalysis, spintronics, and advanced nano-electronic applications [11,12].

3. Results and Discussion

3.1. Band Structure and DOS Analysis of Modified Graphene Systems

The band structure and Density of States (DOS) plots of Pristine Graphene were calculated using Density Functional Theory using Quantum Espresso and are shown in the figure 1.

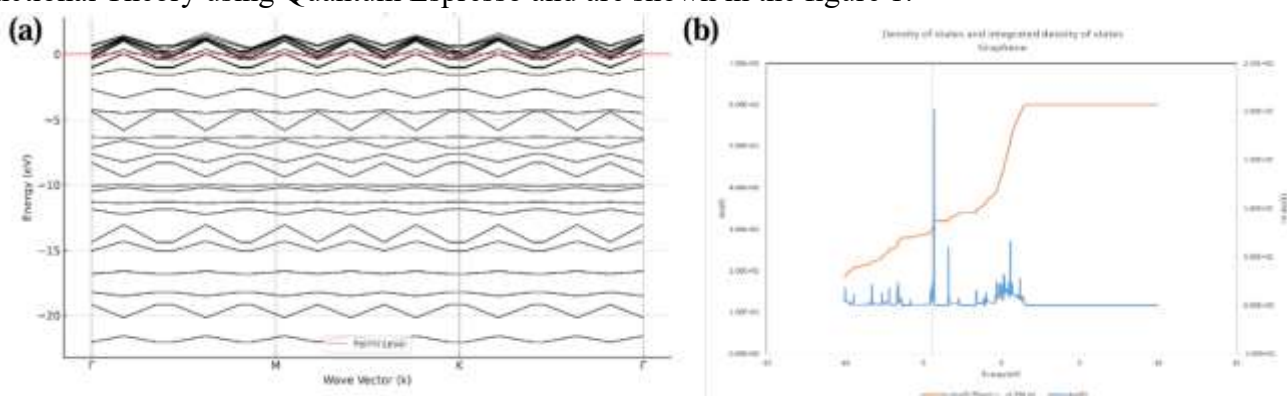


Figure 1. (a) Electronic band structure of graphene calculated using Density Functional Theory (DFT). (b) Total Density of States (DOS) of pristine graphene calculated using Density Functional Theory (DFT) with the PBE exchange–correlation functional.

Pristine graphene shows a linear energy dispersion around the Fermi level ($E_F = -4.398$ eV), with bands crossing at the Dirac point. The density of states is nearly zero at E_F indicating the semi-metallic character

of graphene. This electronic structure lacks a bandgap, which limits its ability to generate photo-induced charge carriers under visible light. Due to the absence of a bandgap and low DOS at E_F , pristine graphene is not ideal as a standalone photocatalyst [13, 14].

The band structure and Density of States (DOS) plots of Boron Doped Graphene are shown in the figure 2. The band structure of B-doped graphene exhibits a clear downward shift in the Fermi level ($E_F = -4.814$ eV) and the appearance of flatter energy bands near E_F . These flatter bands are indicative of the formation of localized acceptor states introduced by boron substitution, which disrupts the sublattice symmetry of the graphene lattice and perturbs the delocalized π -electron network. The corresponding DOS plot shows a significant increase in states near the valence band edge, supporting the assignment of p-type doping behavior [15, 16]. This modification alters the carrier dynamics within the graphene sheet, leading to an increased hole concentration and an enhanced oxidation potential, both of which are beneficial for photocatalytic activity. The introduction of these acceptor levels lowers the energy required to excite electrons across the Fermi level, thereby improving visible-light absorption [17]. Thus, boron doping effectively modulates the electronic structure of graphene, introducing new energy states that facilitate light-induced charge generation and separation. This makes B-doped graphene more active under visible light, promoting hole-driven photocatalytic processes such as dye degradation.

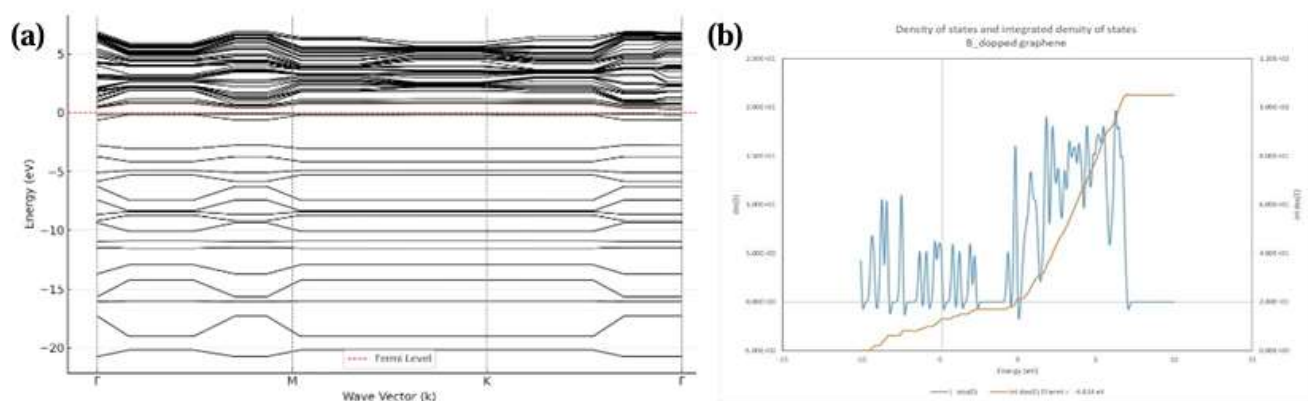


Figure 2. (a) Electronic band structure of B doped graphene calculated using DFT. (b) Total DOS of B-doped graphene obtained from DFT calculations.

The band structure and Density of States (DOS) plots of Nitrogen Doped Graphene are shown in the figure 3.

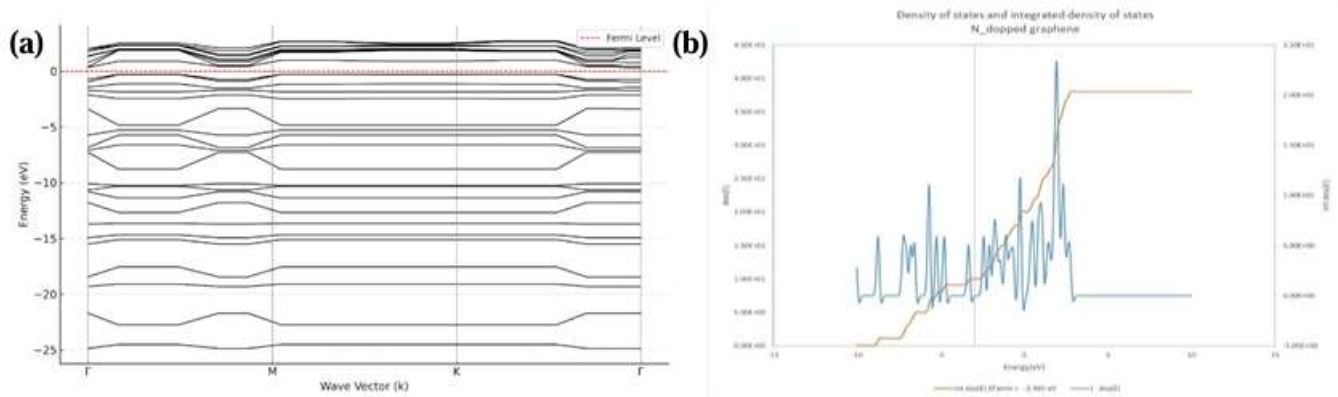


Figure 3. (a) Electronic band structure of N-doped graphene calculated using DFT. (b) Total DOS of N-doped graphene obtained from DFT calculations.

Nitrogen doping alters the electronic structure of graphene by introducing electron-rich donor states near the conduction band. The band structure reveals a distinct upward shift in the Fermi level ($E_F = -2.960$ eV), confirming n-type doping characteristics. The band structure shows distortion and broadening near the Dirac cone, with band tailing near the Fermi level. These changes reflect the donation of electrons from nitrogen to the π -conjugated system of graphene, enhancing electron carrier density [18, 19]. Thus, N-doping increases the electrical conductivity of graphene and favors photocatalytic reduction reactions, particularly in dye degradation. The tailored band alignment facilitates visible-light absorption and enhances the lifetime of photo-generated electrons [20].

The band structure and Density of States (DOS) plots of Cobalt Doped Graphene are shown in the figure 4. Cobalt doping leads to substantial changes in the electronic structure of graphene. The band structure for Co-doped graphene shows broadened features and the emergence of mid-gap states due to strong hybridization between Co d-orbitals and graphene π -electrons. The Fermi level shifts to -3.912 eV, indicating partial electron transfer and metallic character [21]. The band structure reveals flat bands and split states near E_F suggesting the localization of charge carriers and formation of new active sites. Thus, Co-doping introduces chemically active sites that are essential for catalytic activity. The mid-gap states and enhanced charge separation improve the photocatalytic performance of the graphene under visible light irradiation [22].

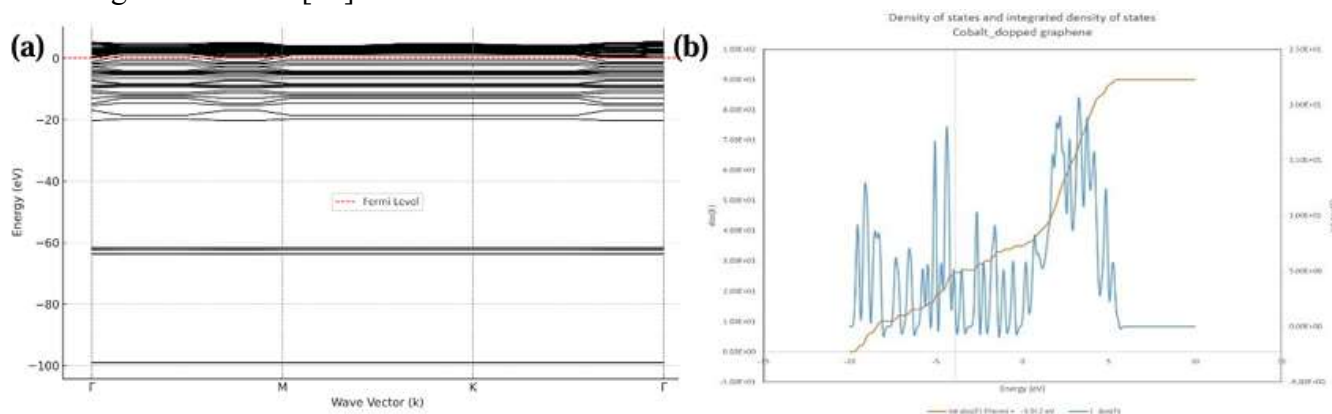


Figure 4. (a) Electronic band structure of cobalt doped graphene calculated using DFT. (b) Total DOS of Cobalt doped graphene obtained from DFT calculations.

The table 1. summarizes the electronic structure and photocatalytic implications for each system.

System	E_F (eV)	Doping Type	Band Feature	Photocatalytic Impact
Pristine Graphene	-4.398	None	Linear dispersion	Inactive due to zero bandgap
B-doped Graphene	-4.814	p-type	Flat bands near valence edge	Enhanced hole generation
N-doped Graphene	-2.960	n-type	Dispersed conduction bands	Improved conductivity and charge transport
Cobalt-doped Graphene	-3.912	Metallic Site	Mid-gap states, band splitting	Strong light absorption and active sites

Table 1. Comparison of different graphene systems obtained from present study.

3.2. Charge Density Mapping and Photocatalytic Implications

To better understand the electronic distribution and bonding characteristics in pristine and modified graphene systems, charge density isosurface plots were generated based on the electron density cube files obtained from Quantum ESPRESSO calculations. The charge density isosurface plots of pristine graphene, boron, nitrogen and cobalt doped graphene are shown in the figure 5. These contour maps provide insight into the localization or delocalization of electrons, which is crucial for interpreting photocatalytic behavior.

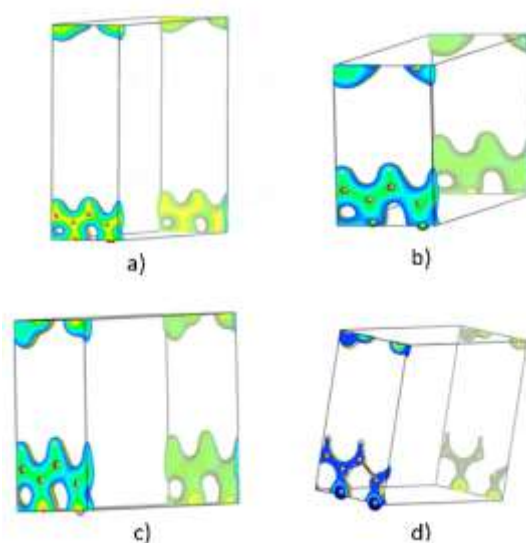


Figure 5. Charge Density Iso-surface Plots of graphene systems: a) Pristine Graphene, b) B doped Graphene, c) N doped Graphene and d) Co doped Graphene.

As shown in Figure 5. (a), pristine graphene displays a highly uniform and delocalized charge distribution. The smooth contouring around carbon atoms confirms π -bond conjugation within the sp^2 -hybridized hexagonal lattice, consistent with prior DFT studies [13]. However, the absence of any notable charge localization or distortion highlights graphene's inherent photocatalytic limitation: minimal active sites for redox reactions [14]. The B-doped graphene system (Figure 5. (b)) shows noticeable distortion in the charge density distribution near the boron dopant site. There is a clear depletion of electron density around the B atom, creating localized charge holes which act as acceptor states. This is characteristic of p-type doping, which enhances the hole concentration and the oxidizing potential of the material, as also supported by earlier reports [16]. Such features increase photocatalytic activity by facilitating hole-driven oxidation mechanisms. As shown in Figure 5. (c), the nitrogen-doped graphene exhibits a significant accumulation of electron density near the N atom. The elevated local charge density is attributed to nitrogen's higher electronegativity, which donates lone pair electrons into the graphene network. This donor-like behavior introduces n-type conductivity and supports enhanced photocatalytic reduction activity by making electrons more readily available for surface reactions [18]. Figure 5. (d) reveals strong electron localization around the cobalt doping site, forming lobed isosurfaces that indicate d-orbital interactions. These mid-gap states enhance visible light absorption and facilitate surface catalysis. Co serves as a charge trap, promoting charge separation and prolonging the lifetime of photoexcited carriers [21, 22]. These active catalytic centers are advantageous for dye degradation and water splitting reactions.

3.3. Electronic Structure of TiO_2 and Graphene/ TiO_2 Systems

To understand the photocatalytic enhancement observed in TiO_2 /graphene heterostructures, a comparative

electronic structure analysis was conducted using Density Functional Theory (DFT). The investigation covers band structure, density of states (DOS), and charge density mapping for pristine TiO_2 and graphene-adsorbed TiO_2 systems.

3.3.1 Band Structure Analysis

The band structure of pristine TiO_2 is shown in Figure 6. (a). A clear bandgap is visible between the valence band maximum and conduction band minimum, indicating its semiconducting nature. The calculated Fermi level lies at 9.829 eV, and the indirect bandgap is approximately 3.2 eV, consistent with experimental values for anatase TiO_2 [23, 24]. This wide bandgap confirms that TiO_2 is primarily UV-active and inefficient under visible light.

In contrast, the band structure of the graphene/ TiO_2 nanocomposite (Figure 6. (b)) reveals significant changes. New energy bands appear near or intersecting the Fermi level (set at -1.045 eV), reflecting the incorporation of graphene π states. These bands reduce the effective bandgap and indicate possible electron delocalization across the graphene– TiO_2 interface. This band structure modification is crucial for enhancing photocatalytic activity under visible light by enabling better charge mobility and absorption [25].

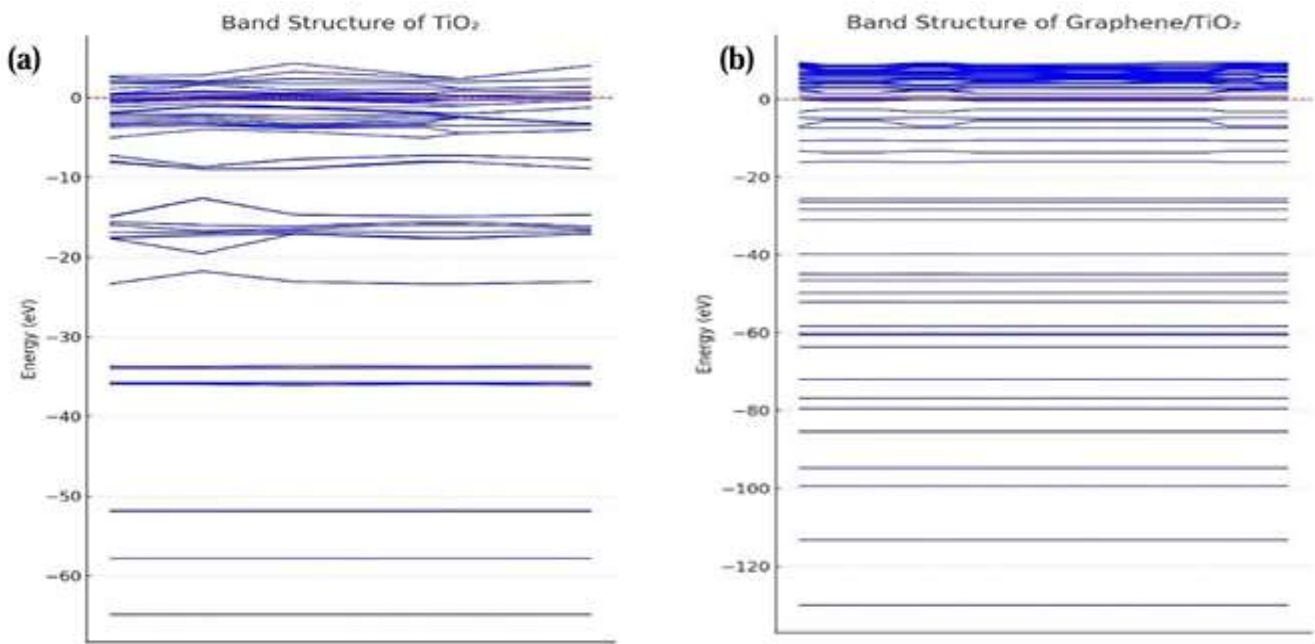


Figure 6. Electronic band structure of (a) TiO_2 and (b) Graphene/ TiO_2 calculated using DFT.

3.3.2 Density of States (DOS) Analysis

The total DOS of pristine TiO_2 (Figure 7. (a)) shows no states in the bandgap region and well-separated valence and conduction bands. The Fermi level lies close to the conduction band, suggesting a low density of free carriers under normal excitation conditions. This electronic arrangement results in limited photocatalytic efficiency due to poor light absorption and fast recombination rates of charge carriers. In the graphene/ TiO_2 heterojunction (Figure 7. (b)), the DOS plot shows the emergence of mid-gap states and a shift in the Fermi level to -1.045 eV, indicating effective charge transfer between graphene and TiO_2 . These new states within the bandgap act as stepping stones for electron excitation and enhance the light absorption spectrum toward the visible region. Such electronic coupling at the interface facilitates electron–hole separation and boosts photocatalytic performance [26].

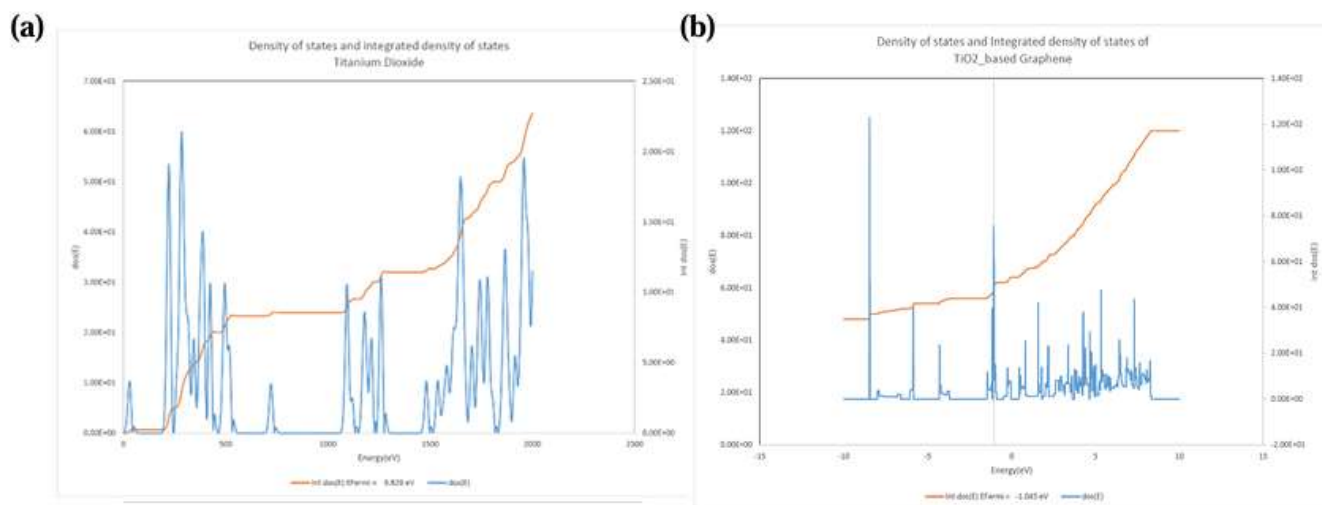


Figure 7. (a) DOS plot of TiO₂ calculated using DFT. (b) DOS plot of Graphene/TiO₂ calculated using DFT.

3.3.3. Charge Density Mapping

The charge density distribution of the pristine TiO₂ system (Figure 8. (a)) reveals a distinctly ionic bonding character, as evidenced by the strong localization of electronic density around the oxygen atoms and notable depletion in the interstitial regions between titanium and oxygen. This reflects the substantial electronegativity difference between Ti and O, resulting in limited orbital overlap and a lack of covalent bonding features. Such a distribution signifies that photogenerated charge carriers in TiO₂ are prone to rapid electron–hole recombination, limiting its intrinsic photocatalytic efficiency under visible light irradiation unless energetically promoted by UV photons [27]. In contrast, the graphene/TiO₂ heterosystem (Figure 8. (b)) exhibits a striking redistribution of electron density at the interface. The charge density isosurface demonstrates enhanced electron accumulation near the graphene–TiO₂ boundary, consistent with interfacial charge delocalization and strong electronic coupling between the π -electron system of graphene and the Ti 3d orbitals of TiO₂. This interfacial redistribution indicates spontaneous electron migration from TiO₂ to graphene, effectively lowering the Fermi level and confirming that graphene functions as a photoinduced electron sink. This mechanism significantly reduces the recombination rate of photoexcited carriers by spatially separating electrons and holes, thereby increasing the carrier lifetime and photocatalytic performance [22].

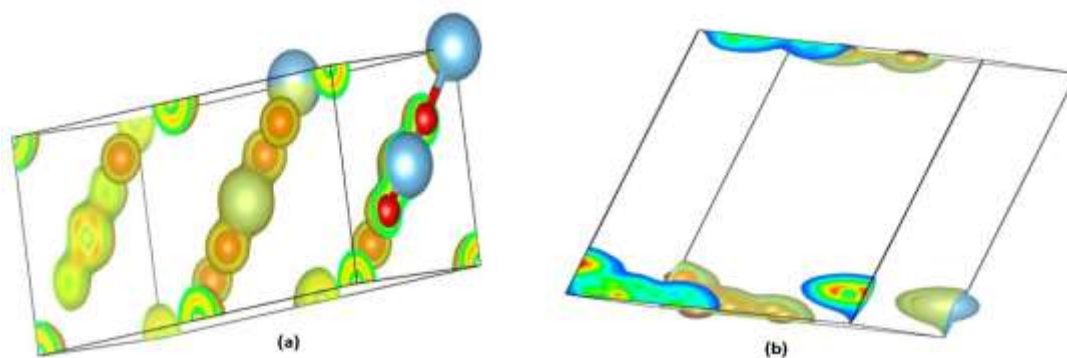


Figure 8. Charge Density Iso-surface Plots of graphene systems: (a) TiO₂ and (b) Graphene/TiO₂.

4. Conclusion

This study demonstrates, through systematic Density Functional Theory (DFT) analysis, how defect engineering and heterostructure formation effectively modulate the electronic structure and photocatalytic potential of graphene-based systems. Pristine graphene, while exhibiting high conductivity, lacks a bandgap and therefore shows limited photocatalytic activity. In contrast, heteroatom doping with boron and nitrogen, as well as cobalt adsorption, significantly alters the Fermi level position, introduces mid-gap states, and enhances charge carrier dynamics. These modifications create active sites that favor visible-light absorption and facilitate charge separation, thereby improving photocatalytic efficiency.

Further, the incorporation of graphene with TiO₂ yields a synergistic heterojunction, where interfacial charge redistribution lowers recombination rates and broadens the absorption spectrum into the visible region. Theoretical results confirm that graphene acts as an electron sink, enhancing charge transport and prolonging carrier lifetimes. This strong coupling between graphene and TiO₂ overcomes the inherent limitations of pristine TiO₂, enabling higher activity under solar irradiation.

References

1. Preetam Datta and Subhasis Roy, "Recent development of photocatalytic application towards wastewater treatment," *Environ. Chem. Lett.*, 2023, 21 (3), 1035–1054.
2. Ahmed Abdelaal, Farzin Banei, Angelo Fenti, Maryam Nili-Ahmadababdi, Miguel Martín-Sómer, and Vahid Keshavarz, "State-of-the-art review of photocatalytic water treatment," *Catalysts*, 2023, 13 (2), 265–289.
3. P. Giannozzi, S. Baroni, N. Bonini, et al., "QUANTUM ESPRESSO: a modular and open-source software project for quantum simulations of materials," *J. Phys.: Condens. Matter*, 2009, 21 (39), 395502.
4. K. S. Novoselov, A. Mishchenko, A. Carvalho, and A. H. Castro Neto, "A roadmap for graphene," *Nature*, 2012, 490 (7419), 192–200.
5. Bo Tang, Haiqun Chen, Haoping Peng, Zhengwei Wang, and Weiqiu Huang, "Graphene modified TiO₂ composite photocatalysts: Mechanism, progress and perspective," *Sci. Total Environ.*, 2018, 622–623, 1342–1359.
6. Ji Hye Lee, Sung Hyun Kwon, Soonchul Kwon, Min Cho, Kwang Ho Kim, Tae Hee Han, and Seung Geol Lee, "Tunable electronic properties of nitrogen and sulfur doped graphene: Density functional theory approach," *Carbon*, 2019, 146, 353–361.
7. P. Giannozzi, S. Baroni, N. Bonini, et al., "QUANTUM ESPRESSO: a modular and open-source software project for quantum simulations of materials," *J. Phys.: Condens. Matter*, 2009, 21, 395502.
8. J. P. Perdew, K. Burke, and M. Ernzerhof, "Generalized Gradient Approximation made simple," *Phys. Rev. Lett.*, 1996, 77 (18), 3865–3868.
9. J. H. Lee, S. H. Kwon, S. C. Kwon, et al., "Tunable electronic properties of nitrogen and sulfur doped graphene: Density functional theory approach," *Carbon*, 2019, 146, 353–361.
10. J. Xie, S. Li, X. Li, et al., "Cobalt-doped graphene for high performance electrocatalysis," *Nano Res.*, 2012, 5 (10), 761–772.
11. K. S. Novoselov, A. K. Geim, S. V. Morozov, et al., "Electric field effect in atomically thin carbon films," *Science*, 2004, 306 (5696), 666–669.
12. H. A. Atwater and A. Polman, "Plasmonics for improved photovoltaic devices," *Nat. Mater.*, 9, 2010, 205–213.
13. A.K. Geim and K. S. Novoselov, "The rise of graphene", *Nat. Mater.* 2007, 6, 183–191.



14. S. Park and R. S. Ruoff, “Chemical methods for the production of graphene”, *Nat. Nanotechnol.*, 2009, 4, 217-224.
15. Kriengkri Timsorn and Chatchawal Wongchoosuk, “Nitrogen-doped graphene quantum sheets for sensing, energy storage and environmental applications”, *J.Compos.Sci.*, 2024, 8 (10) 397-410.
16. Wang Y, Zheng Y, Xu X F, Dubuisson E, Bao Q L, Lu J and Loh K P, “Electrochemical delamination of CVD-grown graphene film: toward the recyclable use of copper catalyst”, *ACS Nano*, 2011, 5 9927–33
17. Haibo Wang, Chuanjian Zhang, Zhihong Liu, Li Wang, Pengxian Han, Hongxia Xu, Kejun Zhang, Shanmu Dong, Jianhua Yao and Guanglei Cui, “Nitrogen-doped graphene nanosheets with excellent lithium storage properties”, *J. Mater. Chem.*, 2011, 21, 5430-5434
18. Zhao, Liuyan & He, Rui & Rim, George & Pasupathy, “Visualizing Individual Nitrogen Dopants in Monolayer Graphene”, *Science*, 2011, 333. 999-1003.
19. Sanjay R. Dhakate, Kiran M. Subhedar and Bhanu Pratap Singh “Improved electrical conductivity and thermal stability of nitrogen doped graphene for supercapacitor application”, 2015, *RSC Adv.* 5, 43036-43057.
20. Lv, R., Li, Q., Botello-Méndez, A. *et al.* “Nitrogen-doped graphene: beyond single substitution and enhanced molar sensing”, 2012, *Sci. Rep.* 2, 586-564.
21. Feng Z, Li Z, Zhang X, Shi Y, Zhou N, “Nitrogen-Doped Carbon Quantum Dots as Fluorescent Probes for Sensitive and Selective Detection of Nitrite”. *Molecules*, 2017, 22(12), 2061-2071.
22. J Hyun, Jong Chan and Jin, Young Soo, Design guidelines for a high-performance hard carbon anode in sodium ion batteries, *Energy Environ. Sci.*, 2024, 17, 2856-2863.
23. Fujishima and K. Honda, “Electrochemical photocatalysis of water at a semiconductor electrode”, *Nature*, 1972, 238, 37-45.
24. M. Grätzel, “Photoelectrochemical cells”, 2001, *Nature*, 414, 338-345.
25. L. Zhang, J. Zeng, C. Xie, Y. Wang, and J. Zeng, “Plasmon-enhanced photocatalytic activities of Au-TiO₂ nanocomposites for organic dye degradation”, 2010, *ACS Nano* 4, 7303-7309.
26. Q. Xiang, J. Yu, and M. Jaroniec, “Graphene-based semiconductor photocatalysts”, *Chem. Soc. Rev.* 2012, 41, 782-791.
27. Amy L. Linsebigler, Guangquan Lu, John T. Yates Jr., “Photocatalysis on TiO₂ Surfaces: Principles, Mechanisms and Selected results”, *Chem. Rev.* 1995, 95, 3, 735–758.